

Numerical Analysis and Design of Dielectric to Plasmonic Waveguides Couplers

Emanuela Paranhos Lima, Vitaly Félix Rodríguez Esquerre

Abstract—In this work, efficient directional coupler composed of dielectric waveguides and metallic film has been analyzed in details by simulations using finite element method (FEM). The structure consists of a step-index fiber with dielectric core, silica cladding, and a metal nanowire parallel to the core. The results show that an efficient conversion of optical dielectric modes to long range plasmonic is possible. Low insertion losses in conjunction with short coupling length and a broadband operation can be achieved under certain conditions. This kind of couplers has potential applications for the design of photonic integrated circuits for signal routing between dielectric/plasmonic waveguides, sensing, lithography, and optical storage systems. A high efficient focusing of light in a very small region can be obtained.

Keywords—Directional coupler, finite element method, metallic nanowire, plasmonic, surface plasmon polariton.

I. INTRODUCTION

In a dielectric waveguide the diameter of an optical beam is restricted by diffraction limit. This limitation is of the order of the wavelength λ_0/n where λ_0 is wavelength in free space, and n is the refractive index. Therefore, the size of optical devices has limitation and implies preventing from decreasing the beam diameter without any limitation by the wavelength [1].

One way to eliminate this problem is the application of plasmonic structures. In plasmonic area, metallic nanofilms have been highlighted on researches because of their properties when combined with dielectric materials. The confinement of radiation in perpendicular directional to interface, that delimits these two materials is due to the surface plasmon polaritons (SPPs). In the literature, there are many experiments involved in plasmon polariton modes in a thin metal layers.

The project of He et al. [2] is composed of a silicon-on-insulator (SOI) waveguide with silicon core, a silicon dioxide gap, and a gold strip. The length of device is 2.2 μm .

The design of Luo et al. [3] consists of gold isosceles triangle (300 nm base x 750 nm height) placed on top of a silicon waveguide (500 nm x 220 nm) with thin SiO_2 layer to separate gold nanotaper from waveguide (20 nm width).

According to Wieduwilt et al. [4], in addition to the use of noble metals like gold and silver, niobium is a great possibility. The schematic involves a cylindrical rod of fused silica glass (20 μm diameter) surrounded by two layers of

ultrathin niobium (12.5 nm thickness), covered with Al_2O_3 (80 nm thickness) and embedded in a liquid with a predefined refractive index ($n = 1.38$). The operated wavelength is 730 nm.

The work of Tellez-Limon et al. [5] designs gold nanoparticle (100 μm width x 50 μm length x 30 nm height) inserted into a core of silicon (500 nm width x 1200 nm length x 450 nm height) with refractive index equal to $n = 2$ and involved by air.

The optical propagation of SPPs guided along gold nanowire involved by silica glass is studied by Marini [6]. The geometry is cylindrical which propagation length equal to $L = 100\mu\text{m}$ and radius ranging from 50 to 500 nm.

In the proposition of Desiatov et al. [7], a silicon tip (450 nm width x 2 μm length x 250 nm height and 10 nm diameter) coupled on a silicon dioxide waveguide (900 nm width x 250 nm height) is shown.

The structure of Boltasseva et al. [8] is composed by a layer of nickel (width 53 μm) and other of gold (500 nm width x 6 μm height) cut in V-shaped (angle of 70.5°) embedded by vacuum.

Geometry, material properties, and operation wavelength are parameters that influence the propagation length. The proposed schematic in this paper is easy to simulate and adjusts these degrees of freedom for efficiency coupling more than 40% because it is produced using step-index fiber and a metal nanowire parallel to the core. Moreover, the use of SPPs is a promising opportunity to minimize optoelectronic components size, increase processing rates integrating nanoelectronics and nanophotonics, and enable the use of applications in sensing [9], [10], nonlinear optics [11], and photovoltaics [12].

II. SIMULATIONS

Here, we propose a two-dimensional multilayer model assuming translational invariance along the x-direction. Therefore, there are only three non-zero electromagnetic field components: H_z , E_x , and E_y . The calculations of the proposed design use FEM, and the meshes are customized to be more refined on region between core and nanowire. The maximum and minimum element size on that region is 12 and 0.08, respectively. The computational modeling of electromagnetic waves requires some techniques for the wave to be absorbed without reflections by the edge of the domain. Thus, Perfect Matched Layer (PML) is used in simulation to absorb wave avoiding reflections for any frequency, polarization, or incident angle of the incident wave.

The schema consists of a dielectric waveguide, where silica

(SiO₂) is the cladding, and a dielectric material with predefined refractive index is the core. Additionally, there is a metal nanowire with a distance t to the core.

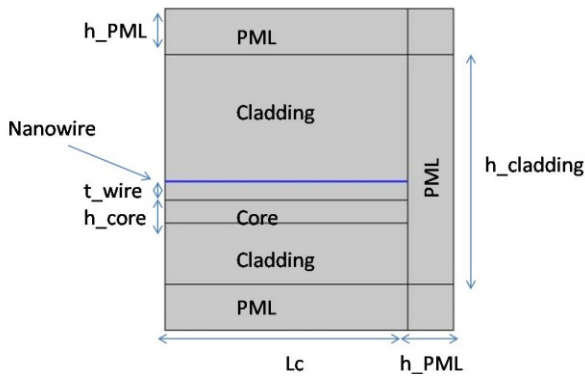


Fig. 1 Scheme of plasmonic directional coupler: Silica cladding, dielectric material core and metal nanowire

According to Tuniz and Schmidt [13], it is possible to determine the device variables using Fig. 2. Initially, in our simulation, we define operation wavelength $\lambda = 1.55 \mu\text{m}$ and gold material of nanowire. For the core refractive index equal to $n = 1.67$ and nanowire width as $w = 25 \text{ nm}$, the diameter of core is equal to $d = 550 \text{ nm}$. For cladding radius, we determine $d = 500 \text{ nm}$, and for the distance between core and nanowire, $t = 300 \text{ nm}$. Then, the parameters are shown in Table I. In simulation, we used extremely fine grids to improve solution of partial differential equations. Port boundary conditions on the core (left) have guaranteed that only TM mode of the waveguide is excited (In-plane vector). An Intel Core i3-2330M CPU at 2.20 GHz and 4 GB RAM memory was used on simulations for approximately 460.000 degrees of freedom wasting around 30 seconds to finish calculations.

The gold refractive index changes in accordance with the operation wavelength. For wavelength $\lambda = 1.55 \mu\text{m}$, according to Rakic et al. [14], the real and imaginary part of permittivity of gold is $\epsilon'_m = -96.958$ and $\epsilon''_m = 11.503$, respectively. Then,

by (1) [15], considering relative permittivity of SiO₂ equal to $\epsilon_d = 3.9$, the coupling length L_c is approximately $0.86 \mu\text{m}$.

$$L_{SPP} = \frac{\lambda}{2\pi} \sqrt{\left(\frac{\epsilon'_m + \epsilon_d}{\epsilon'_m \epsilon_d}\right)^3 \left(\frac{\epsilon'_m{}^2}{\epsilon''_m}\right)} \quad (1)$$

Poynting vector on Fig. 3 confirms the coupling of light at plasmonic nanowire. We can see that energy is transferred to the surface of the gold film over a length $L \approx 400 \text{ nm}$.

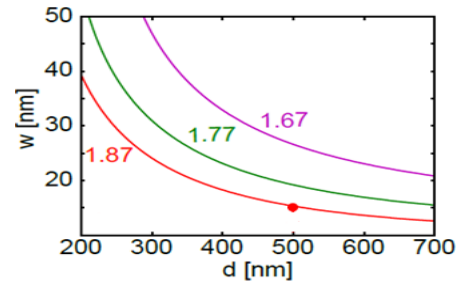


Fig. 2 Graphic of gold nanowire width as function of core thickness for various core refractive indexes [13]

TABLE I PARAMETERS OF SIMULATION	
Parameters	Value
Refractive index, Core	1.67
Refractive index, Cladding	1.44
Height, Nanowire	25 nm
Height, Core	550 nm
Height, Cladding	500 nm
Height, PML	100 nm
Distance, Core & Nanowire	300 nm
Length	2 μm
Wavelength	1.55 μm

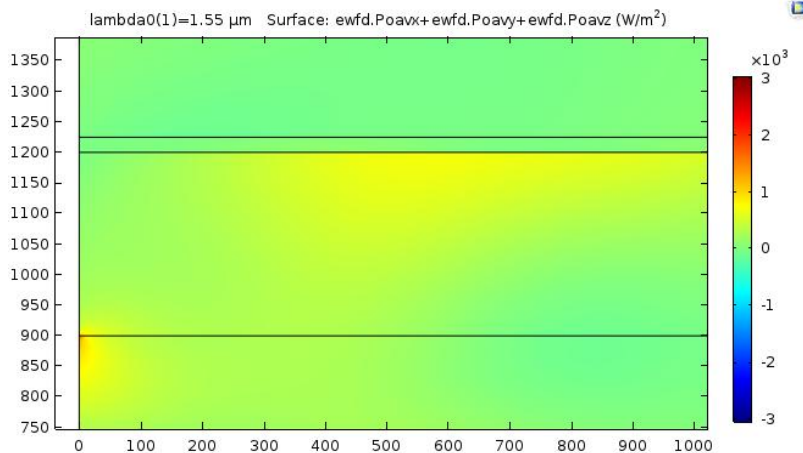


Fig. 3 Power Flow at $\lambda = 1.55 \mu\text{m}$ with $t = 300 \text{ nm}$ and $n = 1.67$

The energy along the core and the nanowire is measured to guarantee that coupling is occurring. One line is established in the middle of the core and other in the middle of the nanowire.

For wavelength $\lambda = 1.55 \mu\text{m}$, the energy versus length graph shows that efficiency is around $\eta = 30.77\%$ ($80 / (180+80) \times 100\%$) at $L_c \approx 400 \text{ nm}$.



Fig. 4 Energy versus length in center of gold nanowire (green) and in center of core (blue) for wavelength $\lambda=1.55 \mu\text{m}$ with $t = 300 \text{ nm}$ and $n = 1.67$

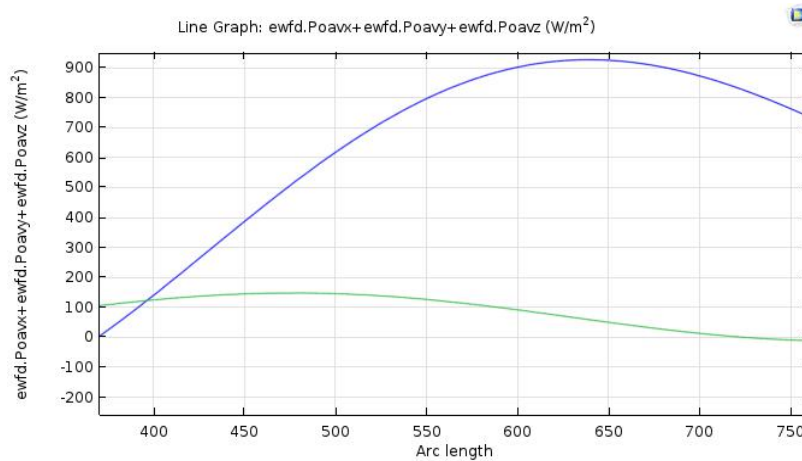


Fig. 5 Energy versus length in center of gold nanowire (green) and in center of core (blue) for wavelength $\lambda=1.55 \mu\text{m}$ with $t = 400 \text{ nm}$ and $n = 1.67$

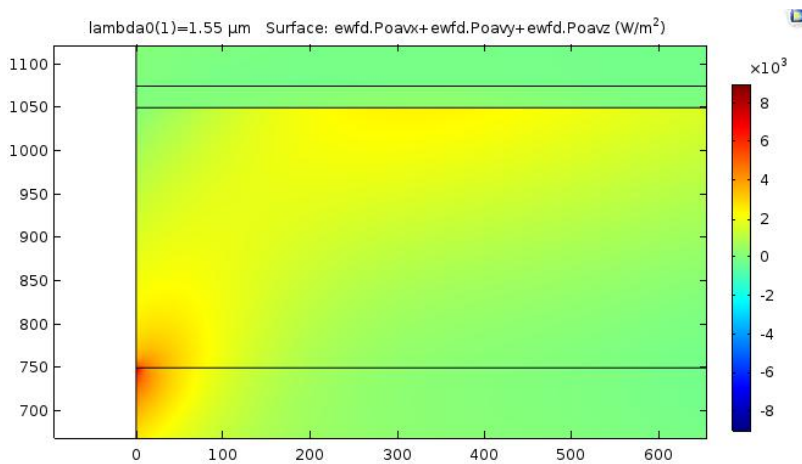


Fig. 6 Power Flow at $\lambda = 1.55 \mu\text{m}$ with $t = 300 \text{ nm}$ and $n = 1.77$

When the distance between metal and core is increased for 400 nm, the efficiency is approximately $\eta = 46.15\%$ ($(120/(140+120)) \times 100\%$) at $L_c \approx 400$ nm as showed on Fig. 5. We

can note that the upper the distance between core and nanowire is the bigger the efficiency.

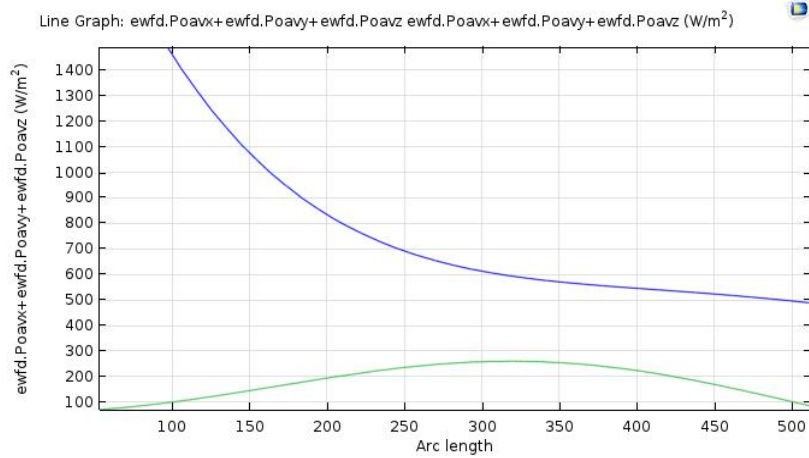


Fig. 7 Energy versus length in center of gold nanowire (green) and in center of core (blue) for wavelength $\lambda=1.55 \mu\text{m}$ with $t = 300$ nm and $n = 1.77$

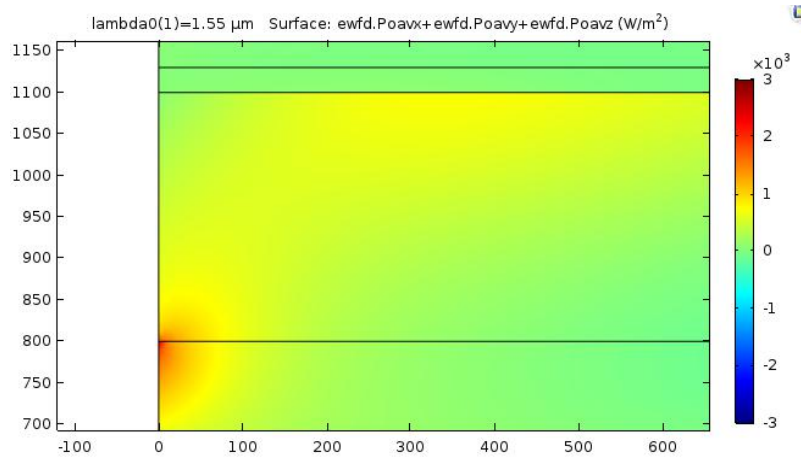


Fig. 8 Power Flow at $\lambda = 1.55 \mu\text{m}$ with $t = 300$ nm, $n = 1.67$ and $d = 450$ nm

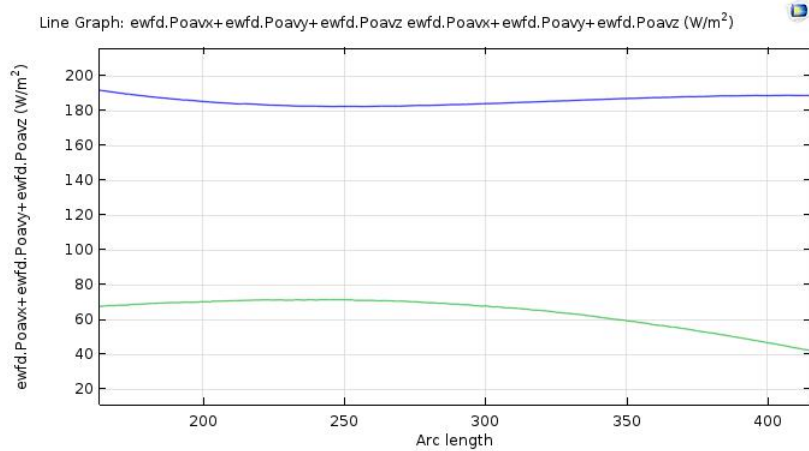


Fig. 9 Energy versus length in center of gold nanowire (green) and in center of core (blue) for wavelength $\lambda=1.55 \mu\text{m}$ with $t = 300$ nm, $n = 1.67$ and $d = 450$ nm

We now investigate the effect of core refractive index. For $n = 1.77$ and nanowire width as $w = 25$ nm, the diameter of core is equal $d \approx 400$ nm as shown in Fig. 2. In this scenario, as demonstrated Fig. 7, the amplitude is bigger than when we use $n = 1.67$ but efficiency is a little lower $\eta = 20.00\%$ ($200/200+800 \times 100\%$) at $L \approx 200$ nm. So, we notice that the lower core refractive index the bigger is the efficiency.

Analyzing a schematic which thickness of nanowire is increased to $w = 30$ nm (keeping $n = 1.67$), from Fig. 2, the diameter of core is $d \approx 450$ nm.

The energy versus length graphic is plotted and show on Fig. 9. The efficiency is around $\eta = 28.00\%$ ($70 / (180+70) \times 100\%$) at $L_c \approx 200$ nm.

III. CONCLUSION

Using the computational approaches, we show that the structure has a good efficiency (more than 40%) on transfer energy from core to metallic nanowire. The results are optimized by choosing a wavelength at $\lambda = 1.55$ μm with $t = 400$ nm and $n = 1.67$. We show also that electromagnetic field confinement increases when thickness of metal thin layer decreases.

For future works, the use of ultrathin niobium films is a promising alternative because of the unique and advantageous properties when compared to noble metals traditionally like gold and silver. Different geometries for nanowire and waveguide are also other lines of studies. Plasmonic nanofocusing properties are a promise by allowing, for example, nanoscale light sources and optical imaging resolution.

REFERENCES

- [1] J. Takahara, S. Yamagishi, H. Taki, A. Morimoto, and T. Kobayashi, "Guiding of a one-dimensional optical beam with nanometer diameter", *Optics Letters*, 1997, Vol. 22, No.7.
- [2] X. He, L. Yang and T. Yang, "Optical nanofocusing by tapering coupled photonic-plasmonic waveguides", *Optics Express*, 2011.
- [3] Y. Luo, M. Chamanzar, A. Apuzzo, R. Salas-Montiel, K. N. Nguyen, S. Blaize and A. Adibi, "On-Chip Hybrid Photonic-Plasmonic Light Concentrator for Nanofocusing in an Integrated Silicon Photonics Platform", *Nano Letters*, 2015.
- [4] T. Wieduwilt, A. Tuniz, S. Linzen, S. Goerke, J. Dellith, U. Hübner and M. A. Schmidt, "Ultrathin niobium nanofilms on fiber optical tapers – a new route towards low-loss hybrid plasmonic modes", *Scientific Reports*, 2015.
- [5] R. Tellez-Limon, B. Bahari, L. Hsu, J. H. Park, A. Kodigala and B. Kanté, "Integrated metaphotonics: symmetries and confined excitation of LSP resonances in a single metallic nanoparticle", *Optics Express*, 2016.
- [6] A. Marini, M. Conforti, G. Della Valle, H. W. Lee, Tr. X. Tran, W. Chang, M. A. Schmidt, S. Longhi, P. St. J. Russell and F. Biancalana, "Ultrafast nonlinear dynamics of surface plasmon polaritons in gold nanowires due to the intrinsic nonlinearity of metals", *New Journal of Physics*, 2013.
- [7] B. Desiatov, I. Goykhman and U. Levy, "Plasmonic nanofocusing of light in an integrated silicon photonics platform", *Optic Express*, 2011.
- [8] A. Boltasseva, V. S. Volkov, R. B. Nielsen, E. Moreno, S. G. Rodrigo and S. I. Bozhevolnyi, "Triangular metal wedges for subwavelength plasmon-polariton guiding at telecom wavelengths"
- [9] H. Gao, J.-C. Yang, J. Y. Lin, A. D. Stuparu, M. H. Lee, M. Mrksich and T. W. Odom, "Nano Lett.", 2010.
- [10] M. Alavirad, L. Roy and P. Berini, "IEEE J. Sel. Top. Quantum Electron", 2014.
- [11] M. Hentschel, T. Utikal, H. Giessen and M. Lippitz, "Nano Lett.", 2012.

- [12] H. A. Atwater and A. Polman, "Plasmonics for improved photovoltaic devices", *Nat. Mater.*, 2010.
- [13] A. Tuniz and M. A. Schmidt, "Broadband efficient directional coupling to short-range plasmons: towards hybrid fiber nanotips", *Optics express*, 2016.
- [14] A. Rakic, A. Djuricic, J. Elazar, and M. Majewski, "Optical properties of metallic films for vertical-cavity optoelectronic devices", *Appl. Opt.* 37, 1998.
- [15] R. Bratiffich, "Fabricação e caracterização de nanoestruturas metálicas para aplicações em dispositivos plasmônicos", Master Degree Theses, Instituto de Física de São Carlos, Universidade de São Paulo, 2015.